Hindawi
Geofluids
Volume 2018, Article ID 5836293, 11 pages
https://doi.org/10.1155/2018/5836293

Research Article

Effects of Formation Dip on Gas Production from Unconfined Marine Hydrate-Bearing Sediments through Depressurization

Yilong Yuan, Tianfu Xu, Yingli Xia, and Xin Xin

Key Laboratory of Groundwater Resources and Environment, Ministry of Education, Jilin University, Changchun 130021, China

Correspondence should be addressed to Xin Xin; xxxx@jlu.edu.cn

Received 24 October 2017; Revised 30 January 2018; Accepted 13 February 2018; Published 26 June 2018

Academic Editor: Egor Dontsov

The effects of geologic conditions and production methods on gas production from hydrate-bearing sediments (HBS) have been widely investigated. The reservoir was usually treated as horizontal distribution, whereas the sloping reservoir was not considered. In fact, most strata have gradients because of the effects of geological structure and diagenesis. In this study, based on currently available geological data from field measurements in Shenhu area of the South China Sea, the effects of formation dip on gas production were investigated through depressurization using a horizontal well. The modeling results indicate that the strategy of horizontal well is an effective production method from the unconfined Class 2 HBS. The predicted cumulative volume of methane produced at the 1000 m horizontal well was 4.51×10^7 ST m^3 over 5-year period. The hydrate dissociation behavior of sloping formation is sensitive to changes in the reservoir pressure. As in unconfined marine hydrate reservoir, the sloping formation is not conducive to free methane gas recovery, which results in more dissolved methane produced at the horizontal well. The obvious issue for this challenging target is relatively low exploitation efficiency of methane because of the recovery of very large volumes of water. Consequently, the development of the favorable well completion method to prevent water production is significantly important for realizing large scale hydrate exploitation in the future.

1. Introduction

Natural gas hydrate (NGH) is crystalline solid composed of water and gas, typically including CH_4, C_2H_6, C_3H_8, CO_2, and H_2S [1, 2]. In nature, the dominant gas in hydrate is CH_4, which is expected to be a potential energy resource. The exploration results show that hydrates are widely distributed in the permafrost and in deep ocean sediments, where the necessary conditions of low temperature and high pressure exist for hydrate stability [3–5].

Gas production from hydrate-bearing sediments (HBS) could be realized by decomposing solid-state hydrate into fluid phases (e.g., gas and water) [4, 6, 7]. There are three main dissociation methods for gas recovery from the HBS: (1) depressurization [2, 5, 8–10], (2) thermal stimulation [11–13], and (3) the use of hydration inhibitors (such as salts and alcohols), which shifts the pressure-temperature equilibrium conditions to dissociate the hydrate [14]. Past field tests, experimental investigations, and numerical studies indicated that depressurization is the most promising method for gas recovery from the HBS, while the other methods may be suitable for enhancing recovery or reservoir stimulation [2, 4, 7, 8, 15].

Up to now, many countries including the United States, Canada, Japan, India, South Korea, and China have launched extensive investigations and field production tests of the HBS [7, 16, 17]. Recently, significant gas hydrate deposits have been confirmed to exist in Shenhu area of the South China Sea (SCS), and this region was regarded as a potential target area [18–21]. In order to seek the most economically and technically feasible method for gas production from the HBS, numerical simulation for its economic, convenient, and flexible response to complex geological problems was considered as the best way to achieve this objective. Based on the available geological data in Shenhu area of the SCS, Zhang et al. [22] investigated the gas production performance by using two parallel horizontal wells to depressurize the HBS; Li et al. [13, 23] and Su et al. [24–26] fully investigated the gas production potential and efficiency through depressurization and the combination of depressurization and

thermal stimulation, respectively, employing both vertical and horizontal wells. Their results indicated low gas production rates and unsatisfied gas/water ratios because of low intrinsic permeability of the HBS and permeable overburden and underburden formations. To accelerate the gas hydrate dissociation and to enlarge the dissociation range, Jin et al. [10] investigated the gas production performance by using the joint depressurization and thermal stimulation based on three horizontal wells. They indicated lower efficiency of hot water injection compared with depressurization. Li et al. [5] and Sun et al. [27] investigated the effects of the permeability of the boundaries on the gas production potential in Shenhu area of the SCS. Their results indicated that the HBS with impermeable boundaries were expected to be the potential gas production target. Huang et al. [9, 28] and Yuan et al. [29] investigated the effects of different geologic conditions on the hydrate dissociation and gas production through depressurization. They indicated that permeability, porosity, and initial hydrate saturation have significant effects on gas production performance. Recently, on the basis of the available geological data from site GMGS3-W19 [20], the geomechanical behaviors for gas production in this area have been conducted and reported by Sun et al. [30]. They indicated that the balance between gas production and reservoir stability is needed to be optimized. The further investigation about the geomechanical behaviors of the HBS induced by gas production indicated that the spatial evolution of the temperature, pore pressure, hydrate saturation, and gas saturation are the most relevant factors [1, 30–35].

The above investigations have properly promoted the development of gas production from the HBS. The effects of production pressure, permeability, porosity, hydrate saturation, thickness, and initial temperature and pressure of HBS on gas production behavior have been widely carried out. Nevertheless, to the best knowledge of the authors, most of previous numerical simulations, the reservoir was usually treated as horizontal distribution, while the sloping reservoir was not considered. In fact, horizontal strata are not common in natural hydrate reservoirs, especially in the marine HBS. Most strata have gradients because of the effects of geological structure and diagenesis [36, 37]. The geologic formation in AT1 site of the Eastern Nankai Trough in Japan with slope angle of approximately 20° is determined based on the interpretations of formation resistivity image logs and drillings [38, 39]. Analysis of seismic and bathymetric data identified seventeen sublinear, near-parallel submarine canyons in Shenhu area of the SCS [19, 40]. The occurrence of gas hydrates was located along the flanks of these prominent canyons; as a consequence, the hydrate reservoirs have a varied dip angles between 6° and 17° in this area [19, 21, 41–43]. Due to influence of the formation dip, the gas production performance and the spatial distribution of reservoir physical characteristics could be different from those of horizontal reservoirs.

This study will look into the effects of the formation dip on the gas production performance in Shenhu area of the SCS, with a horizontal well through depressurization. We designed four simulation schemes with different dip angles of 0° (Base Case), 10° (Case A), 20° (Case B), and 30° (Case C), respectively. In order to make a systematic comparison of the gas production performance in these cases, we used the two criteria, an absolute criterion and a relative criterion [5, 26, 44]. The absolute criterion includes the total methane production rate (Q_{PT}), methane release rate from hydrate dissociation (Q_R), water volumetric production rate (Q_W), and the cumulative volume of methane produced at the well (V_G) and released from hydrate dissociation (V_R). The relative criterion refers to the gas-to-water ratio ($R_{GW} = V_G/V_W$). The reason for considering Q_W and R_{GW} is that the accompanied water production from the borehole will waste a lot of energy and reduce the methane production efficiency. In addition, the practical production characteristics of HBS and multiphase movement behaviors of water and gas induced by depressurization under different dip angles were assessed.

2. Numerical Models and Simulation Approach

2.1. Geological Setting. Shenhu area is located in the Baiyun Sag, Pearl River Mouth Basin (PRMB) of the northern slope of the SCS (Figure 1). Geological, geophysical, geothermal, and geochemical investigations had suggested that Shenhu area is a beneficial district for the formation of NGH [18, 24, 26]. Gas hydrate samples were collected during a recent scientific expedition conducted by the China Geological Survey in this area in May 2007 and September 2015 [5, 19, 20, 45]. The drilling results indicated that the top of the hydrate layers is located 155–229 m below the seafloor (mbsf) and the water depths vary from 1108 m to 1245 m. The thickness of HBS is estimated to be 10–44 m. The average water temperature at the sea floor is measured at about 3.5°C. The in situ salinity measured from the pressure cores is 0.033. The hydrate disseminates in the sediments, mainly composed of fine-grained clay-silts, with the porosity varying from 0.33 to 0.48 and the maximum hydrate saturation of 0.48 [10, 19, 46]. The HBS is overlain and underlain by permeable strata, which have the similar lithology to that in HBS but lack hydrate. Consequently, the geological system of the HBS in this area is typical unconfined Class 2 deposits [10, 47].

2.2. Model Setup

2.2.1. Model Geometry and Spatial Discretization. The geometry of the rectangular 3D system we consider in this study is shown in Figure 2. The model size in x-axis is 200 m, assuming well spacing of 200 m in the future commercial field development with multiwells. The well is perforated in the horizontal part with the length of 1000 m along the y-axis, and the vertical part of the well is sealed to avoid water and gas leaking into the overlying formation and seawater. The thickness of HBS is 40 m, with 30 m overburden and underburden to allow heat exchange with the HBS during a 5-year production period. The 30 m thick boundary layers were sufficient to simulate the boundary effects of heat exchange [8, 17, 26]. The horizontal well is placed at the center of the HBS with a radius of 0.1 m. Assuming uniformity of property and behavior along the horizontal well [5, 32], only a single unit of length ($\Delta y = 1$ m) needs to be simulated.

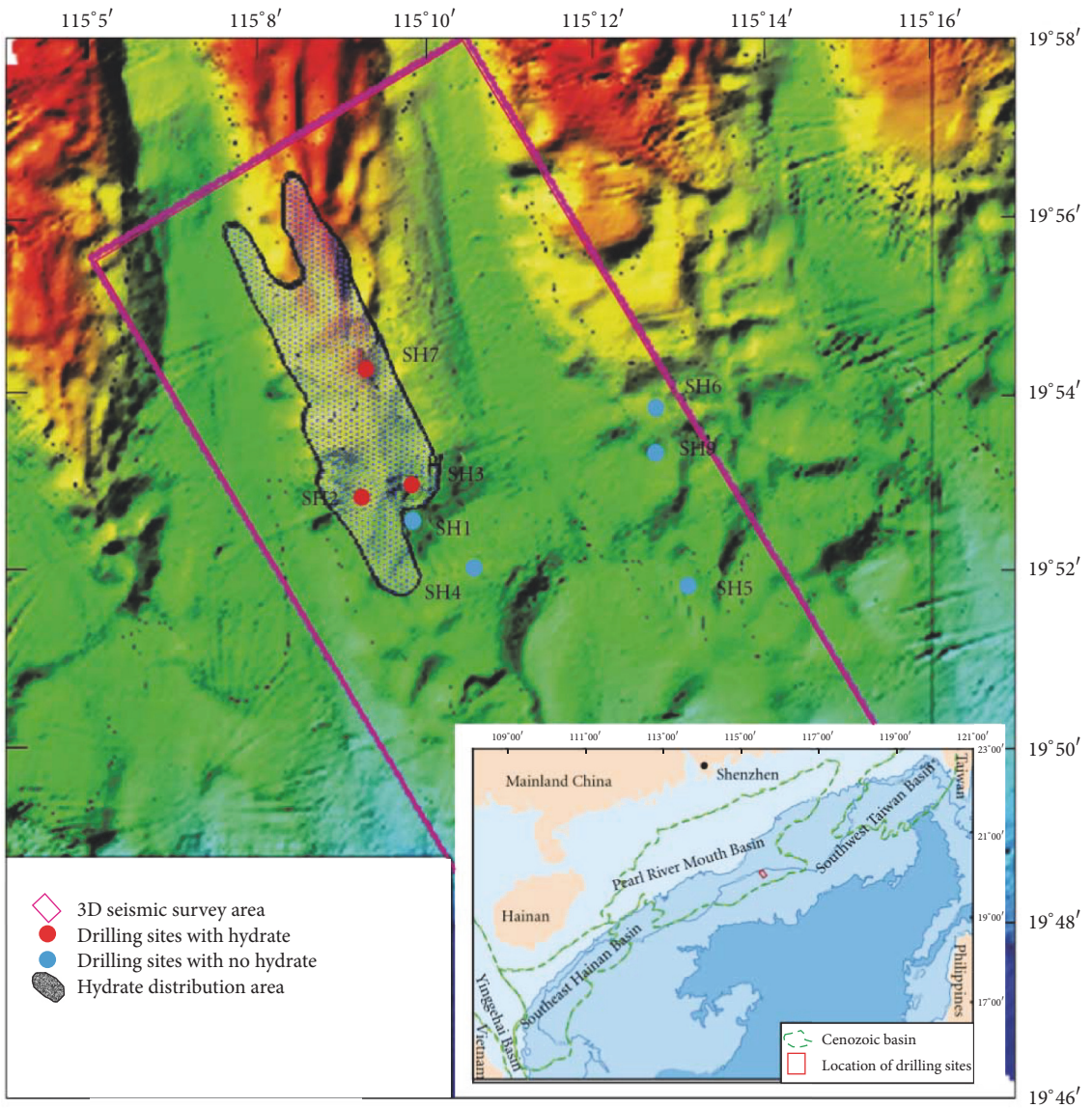

FIGURE 1: Location of study area, drilling sites, and the confirmed gas hydrate distribution in Shenhu area of the SCS [18].

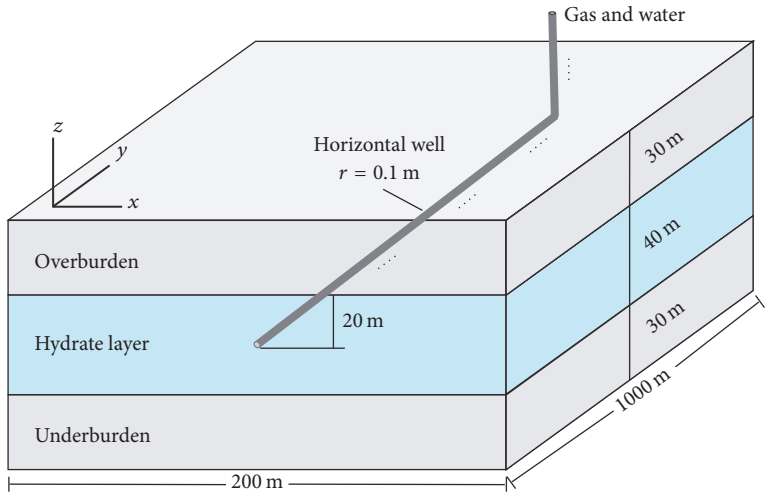

FIGURE 2: Model geometry and the configurations of horizontal well.

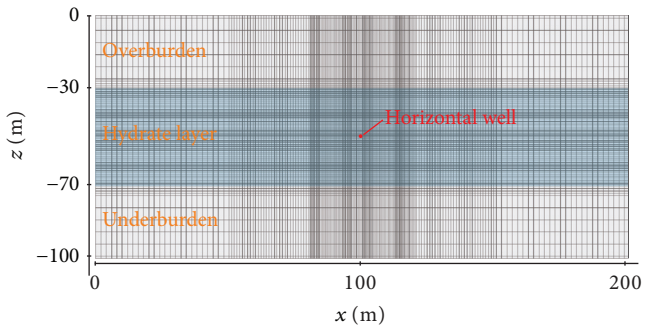

Figure 3: The corresponding grids used in the numerical models, with the location of horizontal well.

Figure 3 shows the corresponding grids used in the numerical models. Previous studies had indicated that the critical processes occur within a limited radius around the horizontal well [1, 4, 32]. Therefore, the grids are refined surrounding the horizontal well with the minimum interval of 0.2 m. The grid size increases with the distance to the well, reaching a size of 2 m at the lateral boundary. Vertical grid size in the HBS is 0.5 m, which gradually increases in both overlying and underlying layers and reaches the maximum size of 5 m.

2.2.2. Reservoir Properties and Parameters. Table 1 presents the main modeling parameters and physical properties for the Shenhu area deposits. These were derived using information gleaned from geophysical well logs and core samples analyses [18, 19, 43, 46]. The initial hydrate saturation is 0.4, which is estimated according to the decrease of chlorinity due to the mixture of fresh water generated by gas hydrate dissociation [46]. The boundary layers of the HBS are saturated by water with a full aqueous saturation of 1.0. The sediment porosity and intrinsic permeability are 0.38 and 1.0×10^{-14} m^2, respectively [10, 26]. To avoid a theoretically correct but computationally intensive solution of the Navier–Stokes equation, the wellbore is simulated as a pseudoporous medium with porosity, permeability, capillary pressure, and low irreducible gas saturation of 1.0, 1.0×10^{-8} m^2, 0 MPa, and 0.005, respectively [4, 5, 48]. Earlier studies had shown the validity of this approximation [8, 49]. The composite thermal conductivity, relative permeability, and capillary pressure models are employed commonly in numerical simulations on gas production from HBS [1, 4, 30–32, 50]. The corresponding parameters for relative permeability and capillary pressure were determined from the field test data by Moridis and Reagan [51]. The changes of effective permeability and capillary pressure are consistent with the porosity and phase saturation during the simulation. With referral to the offshore production test from marine hydrate deposits in the Eastern Nankai Trough of Japan [52], the constant bottom-hole pressure (BHP) P_b is 4 MPa. Consequently, the driving force of the depressurization ΔP is 12 MPa ($\Delta P = P_m - P_b$); P_m is the initial pressure in the HBS at the elevation of the horizontal well (Figure 2).

Table 1: Main model parameters of the HBS in Shenhu area of the SCS.

Parameter	Value
HBS thickness, H	40 m
Porosity, ϕ	0.38
Intrinsic permeability, k	1.0×10^{-14} m^2 (1 mD = 1.0×10^{-15} m^2)
Gas composition	100% CH4
Hydrate saturation in the HBS, S_h	0.40
Water salinity, X_i	3.30%
Pressure at the middle of the HBS, P_m	16.0 MPa
Temperature at the middle of the HBS, T_m	13.95°C
Critical mobile porosity, ϕ_{cri}	0.05
Rock grain density, ρ_R	2600 kg/m^3
Wet thermal conductivity, λ_W	3.1 W/m/K
Dry thermal conductivity, λ_D	1.0 W/m/K
Pore compressibility, α_P	1.0×10^{-8} Pa^{-1}
Bottom-hole pressure, P_b	4 MPa
Composite thermal conductivity model [8]	$\lambda = \lambda_D + \left(S_A^{1/2} + S_h^{1/2}\right)(\lambda_W - \lambda_D) + \phi S_I \lambda_I$
Capillary pressure model [53]	$P_{\text{cap}} = -P_0([S_A^*]^{-1/m} - 1)^{1/m}$ $S_A^* = \dfrac{(S_A - S_{irA})}{(S_{mxA} - S_{irA})}$
S_{mxA}	1.0
m	0.45
P_0	1.0×10^5 Pa
Relative permeability model [1]	$k_{rA} = (S_A^*)^{n_A}$ $k_{rG} = (S_G^*)^{n_G}$ $S_G^* = \dfrac{(S_G - S_{irG})}{(1 - S_{irA})}$
n_A	3.572
n_G	3.572
S_{irA}	0.30
S_{irG}	0.02

2.2.3. Initial and Boundary Conditions. The initial formation pressure was specified in accordance with the hydrostatic pressure, which was computed according to the water depth and a pressure-adjusted saline water density [50]. Figure 4 shows the resultant initial pressure distribution of different dip angles. To the sloping formations, there will be an angle (e.g., equal to the formation dip) between the initial pressure contour lines and the strata lines. The initial temperature was specified to be 3.5°C at the seafloor [5, 46]. The temperature

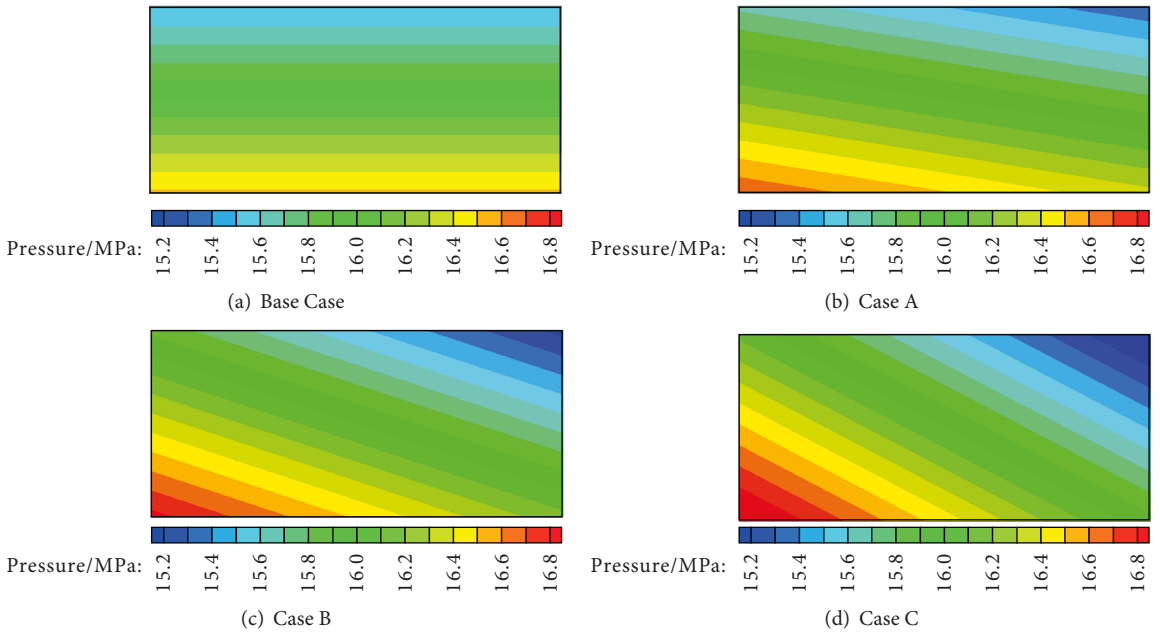

Figure 4: Cross section showing the initial pressure distribution: (a) Base Case with dip angle of 0°, (b) Case A with dip angle of 10°, (c) Case B with dip angle of 20°, and (d) Case C with dip angle of 30°.

profile was assigned to vary linearly as a function of depth with a geothermal gradient of 47°C/km [10, 18, 26, 46].

Because of symmetry of the horizontal strata, there is no flow of fluids and heat through the lateral boundaries. For the inclined formation, there exists the lateral boundary fluid and heat flow due to the acceleration of gravity. However, the hydrate dissociation zone is limited around the production well for the specified unconfined Class 2 HBS (e.g., the dissociation radius is no more than 30 m); thus, the lateral boundary flow has insignificant influence on gas production from hydrate reservoir (e.g., verified by the sensitivity study). Consequently, for both the horizontal strata and inclined formation, no flow of fluids and heat are specified for the lateral boundaries [32]. Because the boundary layers have similar lithology to that in HBS, the top and bottom boundaries are designed as constant temperature and pressure boundaries [50].

2.2.4. The Numerical Simulation Code. In this numerical study, we use TOUGH + HYDRATE to investigate the effects of formation dip on gas production performance from the marine HBS. This code can model the nonisothermal hydration reaction, multiphase behavior, and flow of fluids and heat under conditions typical in geological media containing gas hydrates [4, 6]. It includes both an equilibrium and a kinetic model of hydrate formation and dissociation. These models cover four phases (i.e., gas, aqueous, ice, and hydrate) and four mass components (i.e., H_2O, CH_4, hydrate, and water-soluble inhibitors such as salts or alcohols) with each component existing in each phase [6].

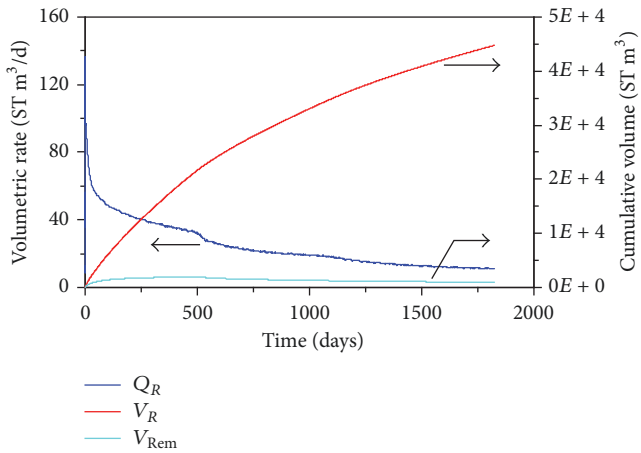

Figure 5: Evaluation of methane release rate (Q_R), the cumulative volume of methane released in the reservoir (V_R), and the cumulative volume of methane remaining in the reservoir (V_{Rem}) during gas production from horizontal strata.

3. Simulation Results and Discussions

3.1. Production Behaviors of Horizontal Strata. The extraction of fluid (e.g., gas and water) from the horizontal well leads to depressurization-induced hydrate dissociation in the HBS. Figure 5 shows the evolution of methane release rate (Q_R), the cumulative volume of methane released from hydrate dissociation (V_R), and the cumulative volume of methane remaining in the reservoir (V_{Rem}) over 5-year period. In this section, all of the following plotted results reveal the unit section (1 m) of horizontal well.

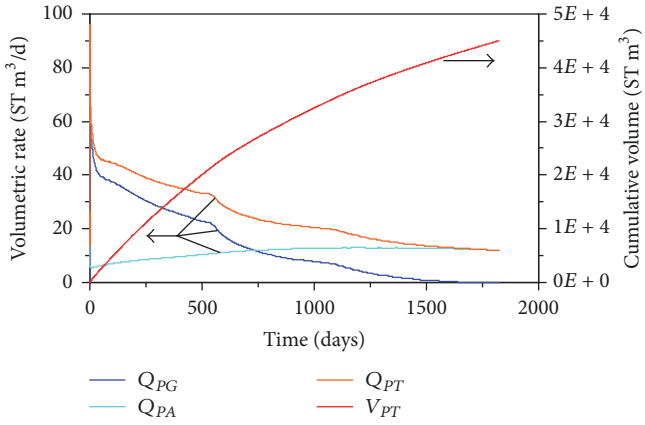

Figure 6: Evaluation of methane gas production rate (Q_{PG}), the dissolved methane production rate (Q_{PA}), the total methane production rate (Q_{PT}), and the cumulative methane volume produced at the well (V_{PT}) during gas production from horizontal strata.

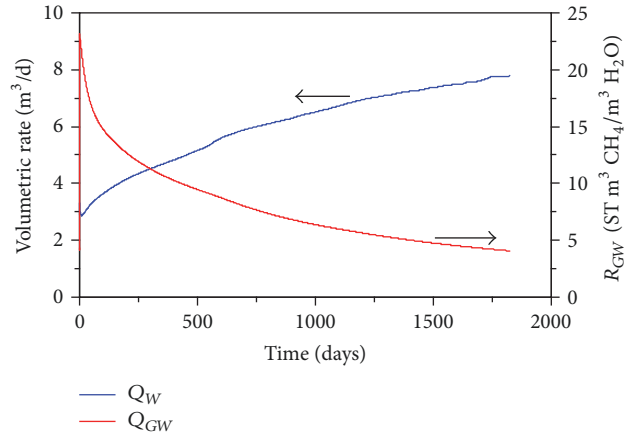

Figure 7: Evaluation of water volumetric production rate (Q_W) and the gas-to-water ratio (R_{GW}) during gas production from horizontal strata.

As shown in Figure 5, the constant depressurization at the well results in an initial burst of gas release in the vicinity of the horizontal well. Consequently, the maximum Q_R occurs at the initial point with the value of approximately 136 ST m^3/d. This phenomenon is usually called "gas cavity" [23, 54]. This is because the drastic decrease of fluid pressure in hydrate reservoir causes the significant hydrate dissociation, resulting in an immediate increase of Q_R. Meanwhile, the massive gas released from hydrate dissociation results in reservoir pressure increase abruptly, which limits the hydrate dissociation rate significantly. After the incident of "gas cavity," Q_R rapidly drops at the early stage and gradually decreases with a slowing decline rate. This is mainly because (1) the low effective permeability of hydrate reservoir results in the fact that free gas could not be yielded from the HBS timely and, as a consequence, the dissociation front with a high pressure level; (2) the endothermic nature of hydrate dissociation results in a low temperature region around the horizontal well; (3) the function of self-sealing gradually disappears with hydrate dissociation above and below the horizontal well, resulting in the fact that water seepage from boundary layers catches up with the water discharge from the HBS to the borehole. All of these reasons impede the rapid hydrate dissociation in the HBS. At the end of 5-year production period, a total of $V_R = 4.48 \times 10^4$ m^3 have been produced from the methane hydrate dissociation.

Figure 6 shows the evolution of methane gas production rate (Q_{PG}), the dissolved methane production rate (Q_{PA}), the total methane production rate ($Q_{PT} = Q_{PG} + Q_{PA}$), and the cumulative methane volume produced at the well (V_{PT}) over 5-year period. Due to the produced methane mainly from the hydrate dissociation, Q_{PT} changes following the trend of Q_R (Figure 5). As shown in Figure 6, the maximum Q_{PT} occurs at the initial point with the value of approximately 96 ST m^3/d. As expected, Q_{PG} is consistently lower than Q_R because of dissolving in formation water and the need for gas accumulation in the reservoir until the gas saturation overcomes its irreducible level of S_{irG}. Q_{PG} decreases in the whole production stage until no free methane gas is produced from the hydrate reservoir (e.g., $Q_{PG} = 0$). This is because Q_R decreases with time (Figure 5), which results in low gas saturation in the reservoir at the late stage. Meanwhile, the total methane production rate Q_{PT} is low and almost constant at the late stage, because the methane is produced mainly by the dissolved methane (Q_{PA}) exsolution from the formation water. At the end of 5-year production period, a total of $V_{PT} = 4.51 \times 10^4$ ST m^3 have been produced at the unit section (1 m) of horizontal well. Comparing V_{PT} and V_R (Figure 5) indicates that the majority of the produced methane originated from the hydrate dissociation and the additional methane comes from original dissolved methane in the formation water.

Figure 7 shows the evolution of water volumetric production rate (Q_W) and the gas-to-water ratio (R_{GW}) over 5-year period. R_{GW} is a relative criterion for evaluating the methane production efficiency, which is defined as

$$R_{GW} = \frac{\int Q_{PT}\, dt}{\int Q_W\, dt}. \quad (1)$$

As shown in Figure 7, Q_W increases at a decreasing rate and reaches the maximum value of 7.78 m^3/d. This pattern follows a typical water discharge curve in the unconfined aquifer discharged by the well under a constant pressure [10]. The pseudo-steady state at the late stage indicates that the water recharge by the seepage from boundary layers catches up with the water discharge from the HBS to the borehole (Figure 8(b)). Meanwhile, R_{GW} decreases at a decreasing rate which is affected by Q_{PT} and Q_W simultaneously (see (1)). This indicates that the major products output from borehole are methane in the early stage, while water only accounts for a small part. However, as mining continues, water becomes the major product at the late stage, and the methane output decreases to a significant low level (Figure 6). This is mainly because the solid hydrates above and below the horizontal well can temporarily act as sealing layers to prevent water production and free gas escaping from hydrate reservoir into surrounding formations (Figure 8(a)).

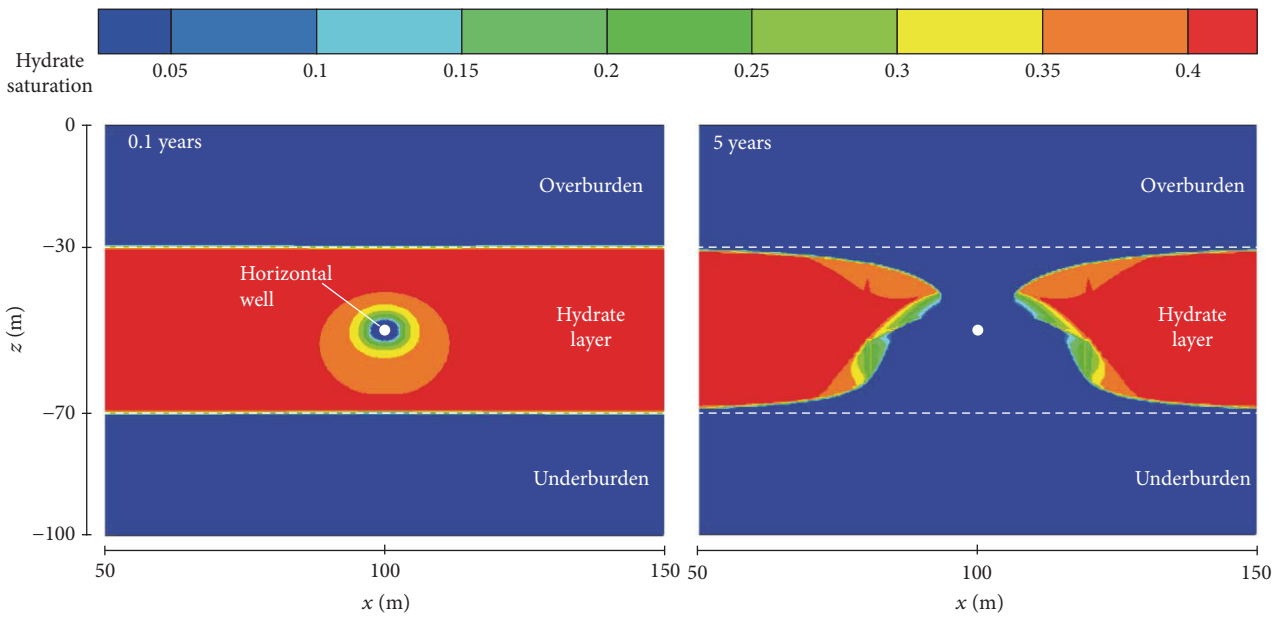

Figure 8: Spatial distribution of hydrate saturation in the reservoir during gas production from the unconfined Class 2 HBS.

However, once the hydrate above and below the horizontal well dissociates completely, the self-sealing function will disappear (Figure 8(b)); as a result, the methane production efficiency (R_{GW}) decreases significantly.

Moridis and Kowalsky [47] had evaluated the gas production potential of such deposits (e.g., unconfined Class 2 HBS) using both single-well and five-spot well configurations. Their results indicated that unconfined Class 2 HBS are among the most challenging targets for methane production because (1) the absence of confining boundaries limits the effectiveness of depressurization, (2) the rate of methane production at the well is much lower (e.g., less than 200 m^3/d), and (3) methane production is accompanied by the production of very large volumes of water. However, the modeling results of this work indicate that the strategy of horizontal well through depressurization is an effective method to exploit the gas hydrate in this unconfined Class 2 HBS. Review of Figure 6 shows that the average methane production rates and the cumulative methane volume produced at the well over 5-year period reach 2.47×10^4 ST m^3/d and 4.51×10^7 ST m^3 over the length of 1000 m horizontal well, respectively. However, the obvious issue is relatively low exploitation efficiency of methane (e.g., R_{GW} shown in Figure 7) because gas production is accompanied by the recovery of very large volumes of water. Consequently, the development of the favorable well completion method to prevent water production is significantly important to realize large scale hydrate exploitation in the future.

3.2. Impact of Formation Dip on Hydrate Production Performance

3.2.1. Gas Release from Hydrate Dissociation. Figure 9 shows the difference of V_R and V_{Rem} between horizontal strata and those sloping formations over the length of 1000 m horizontal well. As shown in this figure, the sloping formation has a higher V_R than that of horizontal strata. When the dip angles change from 0°, to 10°, 20°, and 30°, the cumulative volume of methane released from hydrate dissociation (V_R) increased by 881 ST m^3, 4098 ST m^3, and 10490 ST m^3, respectively. This indicates that the sloping formation causes the gas hydrate in the HBS to be unstable, because the lower half portion of the hydrate reservoir is closer to the bottom of hydrate stability zone (BHSZ). This means that hydrate dissociation behavior of sloping formation is sensitive to changes in the reservoir pressure, which can be used to explain the phenomenon that a

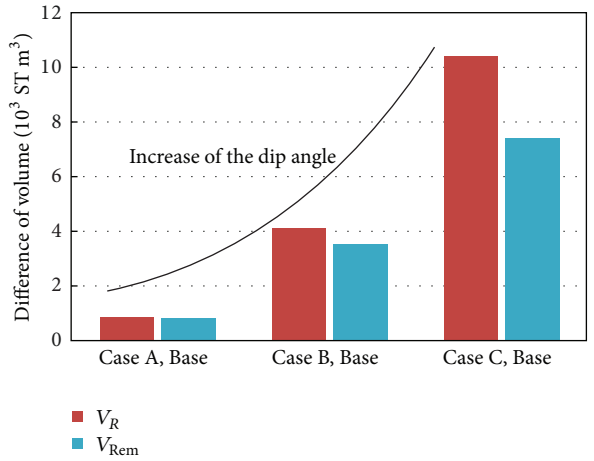

Figure 9: The difference of the cumulative volume of methane released from hydrate dissociation (V_R) and methane remaining in the reservoir (V_{Rem}) between horizontal strata and those sloping formations at the end of 5-year production period.

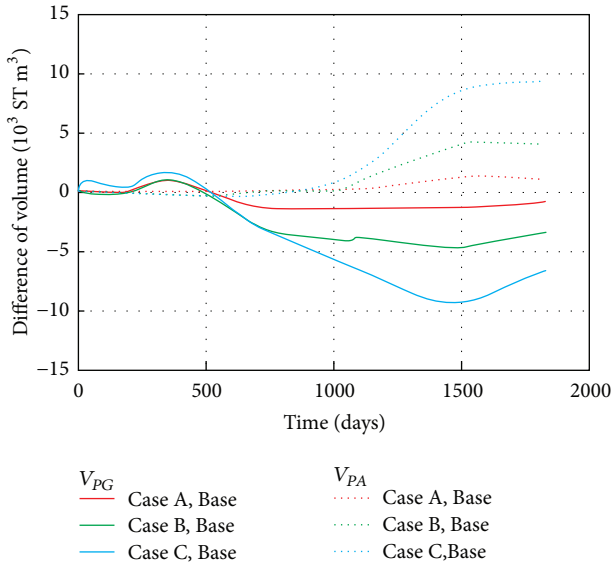

Figure 10: The difference of the cumulative volume of methane gas produced at the well (V_{PG}) and the dissolved methane produced at the well (V_{PA}) between horizontal strata and those sloping formations over 5-year production period.

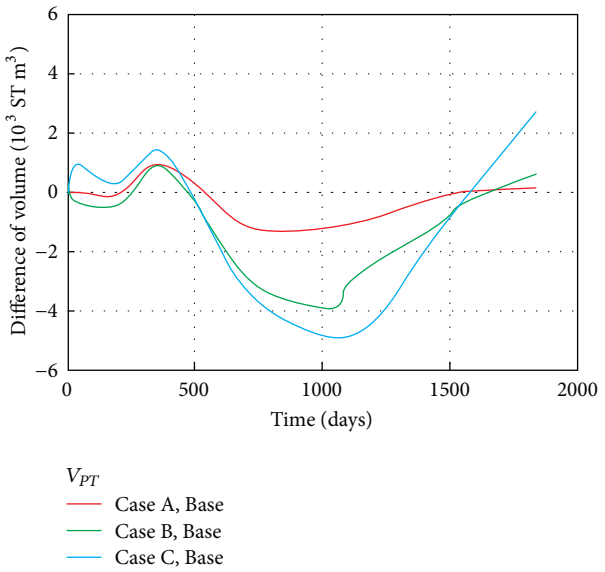

Figure 11: The difference of the cumulative volume of total methane gas produced at the well (V_{PT}) between horizontal strata and those sloping formations over 5-year production period.

large number of marine gases release during geologic activity. In the actual situation, this process is more obvious because of the upper half portion of the hydrate reservoir with rapid decline of pressure, but slightly temperature decreases in a short period of time. On the other hand, the difference of V_{Rem} between horizontal strata and those sloping formations (Figure 9) indicates that the dip angle is not conducive to gas recovery during gas production from the hydrate reservoir. This is because free gas far from the production well is hard to yield from the hydrate reservoir.

3.2.2. Gas Production at the Well. Figure 10 shows the difference of V_{PG} and V_{PA} between horizontal strata and those sloping formations over the length of 1000 m horizontal well. As shown in this figure, the influence of the formation dip on V_{PG} and V_{PA} is quite different, both of which have two stages.

In the first 500 days, the dip angle has very slight effect on V_{PG}, because the available hydrate in the vicinity of the horizontal well has not been exhausted. However, the sloping formation has a lower V_{PG} than that of horizontal strata at the late stage. This further proves that the inclined formation is not conducive to free gas recovery from the unconfined Class 2 HBS. On the other hand, the difference of V_{PA} shows that the dip angle has very slight effect on V_{PA} in the first 1000 days. However, the sloping formation has a higher V_{PA} than that of horizontal strata at the late stage. When the dip angles change from 0°, to 10°, 20°, and 30°, the cumulative volume of V_{PA} increased by 1034 ST m^3, 3988 ST m^3, and 9306 ST m^3, respectively. This is because the methane is produced mainly by the free gas from the hydrate reservoir in the early stage, while, at the late stage, the methane is produced mainly by the dissolved methane exsolution from the formation water (Figure 6).

Figure 11 shows the difference of total methane produced at the well between horizontal strata and those sloping formations over the length of 1000 m horizontal well. The initial oscillation illustrates that the hydrate dissociation behavior of sloping formation is sensitive to changes in the reservoir pressure. With the stability of reservoir pressure, the sloping formation results in a lower V_{PT} than that of horizontal strata. The greater the dip angle, the more significant the maximal difference of V_{PT}. This is because the methane is produced mainly by the free gas (V_{PG}) during this stage and the inclined formation is not conducive to gas recovery from the unconfined Class 2 HBS (Figure 9). However, this situation is reversed at the late stage because the available hydrate in the vicinity of horizontal well is exhausted and the methane is produced mainly by the dissolved gas.

3.2.3. Water Production at the Well. Figure 12 shows the difference of V_W and R_{GW} between horizontal strata and those sloping formations over the length of 1000 m horizontal well. As shown in this figure, the sloping formations yield lower water production compared with the horizontal strata. When the dip angles change from 0°, to 10°, 20°, and 30°, the cumulative volume of V_W decreased by 97 m^3, 777 m^3, and 1554 m^3, respectively. This means that the inclined formation can restrict water from the boundary layers to the production well to some extent. Meanwhile, the sloping formation has a neglected influence on R_{GW} as shown in Figure 12. This is because sloping formation has a slight influence on both V_{PT} and V_W for the unit section (1 m) of horizontal well.

4. Conclusions

In this study, we numerically investigated the effects of the formation dip on gas production from the unconfined marine

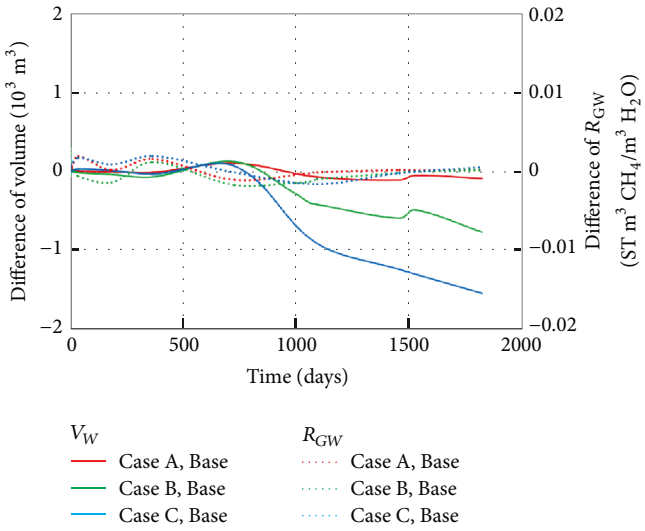

FIGURE 12: The difference of the cumulative volume of water produced at the well (V_W) and gas-to-water ratio (R_{GW}) between horizontal strata and those sloping formations over 5-year production period.

hydrate-bearing sediments (HBS) in Shenhu area of the South China Sea. The present modeling and analysis results are specific to the conditions and parameters considered. Based on the numerical simulations, the following conclusions can be drawn:

(1) The horizontal well configuration through depressurization is an effective production method related to the challenging unconfined Class 2 HBS. The model predicted that the average methane production rates and the cumulative volume produced at the 1000 m horizontal well reach 2.47×10^4 ST m^3/d and 4.51×10^7 ST m^3 over 5-year period, respectively.

(2) The methane is produced mainly by the free gas from the hydrate reservoir in the early stage, while the methane is produced mainly by the dissolved methane exsolution from the formation water at the late stage.

(3) The hydrate dissociation behavior of sloping formation is sensitive to changes in the reservoir pressure. When the dip angles change from 0°, to 10°, 20°, and 30°, the cumulative volume of methane released from hydrate dissociation increased by 881 ST m^3, 4098 ST m^3, and 10490 ST m^3, respectively.

(4) The sloping formation is not conducive to free methane gas recovery from the unconfined Class 2 HBS, which results in more dissolved methane produced at the horizontal well. Consequently, the dip angle is not one of the main parameters that greatly affect the total methane production performance form the unconfined marine hydrate reservoir.

(5) The sloping formation yields lower water production which can restrict water from the boundary layers to the production well to some extent.

(6) As in unconfined Class 2 HBS, the obvious issue is relatively low exploitation efficiency of methane because gas production is accompanied by the recovery of very large volumes of water. Consequently, the development of the favorable well completion method to prevent water production is significantly important to realize large scale hydrate exploitation in the future.

Conflicts of Interest

There are no conflicts of interest of other works related to this paper.

Acknowledgments

This work was supported by the National Program on Key Research and Development Project (no. 2017YFC0307304) and the Graduate Innovation Found of Jilin University (no. 2017018).

References

[1] J. Rutqvist and G. J. Moridis, "Numerical studies on the geomechanical stability of hydrate-bearing sediments," *SPE Journal*, vol. 14, no. 2, pp. 267–282, 2009.

[2] Y. Konno, T. Fujii, A. Sato et al., "Key findings of the world's first offshore methane hydrate production test off the coast of Japan: toward future commercial production," *Energy & Fuels*, vol. 31, no. 3, pp. 2607–2616, 2017.

[3] M. Kurihara, A. Sato, H. Ouchi et al., "Prediction of gas productivity from eastern Nankai trough methane-hydrate reservoirs," *SPE Reservoir Evaluation and Engineering*, vol. 12, no. 3, pp. 477–499, 2009.

[4] G. J. Moridis and M. T. Reagan, "Estimating the upper limit of gas production from Class 2 hydrate accumulations in the permafrost: 2. Alternative well designs and sensitivity analysis," *Journal of Petroleum Science and Engineering*, vol. 76, no. 3-4, pp. 124–137, 2011.

[5] G. Li, X.-S. Li, K. Zhang, B. Li, and Y. Zhang, "Effects of impermeable boundaries on gas production from hydrate accumulations in the shenhu area of the South China sea," *Energies*, vol. 6, no. 8, pp. 4078–4096, 2013.

[6] G. J. Moridis and K. Pruess, *User's manual for the hydrate v1.5 option of TOUGH+ v1.5: a code for the simulation of system behavior in hydrate-bearing geologic media*, LBNL, Berkeley, Calif, USA, 2014.

[7] X. S. Li, C. G. Xu, Y. Zhang, X. K. Ruan, G. Li, and Y. Wang, "Investigation into gas production from natural gas hydrate: a review," *Applied Energy*, vol. 172, pp. 286–322, 2016.

[8] G. J. Moridis, M. B. Kowalsky, and K. Pruess, "Depressurization-induced gas production from class 1 hydrate deposits," *SPE Reservoir Evaluation and Engineering*, vol. 10, no. 5, pp. 458–481, 2007.

[9] L. Huang, Z. Su, N. Wu, and J. Cheng, "Analysis on geologic conditions affecting the performance of gas production from hydrate deposits," *Marine and Petroleum Geology*, vol. 77, pp. 19–29, 2016.

[10] G. Jin, T. Xu, X. Xin, M. Wei, and C. Liu, "Numerical evaluation of the methane production from unconfined gas hydrate-bearing sediment by thermal stimulation and depressurization

in Shenhu area, South China Sea," *Journal of Natural Gas Science and Engineering*, vol. 33, pp. 497–508, 2016.

[11] V. Kamath and S. P. Godbole, "Evaluation of hot-brine stimulation technique for gas production from natural gas hydrates," *Journal of Petroleum Technology*, vol. 39, no. 11, pp. 1379–1388, 1985.

[12] X. S. Li, L. H. Wan, G. Li, Q. P. Li, Z. Y. Chen, and K. F. Yan, "Experimental investigation into the production behavior of methane hydrate in porous sediment with hot brine stimulation," *Industrial & Engineering Chemistry Research*, vol. 47, pp. 9–11, 2008.

[13] G. Li, G. J. Moridis, K. Zhang, and X.-S. Li, "The use of huff and puff method in a single horizontal well in gas production from marine gas hydrate deposits in the Shenhu Area of South China Sea," *Journal of Petroleum Science and Engineering*, vol. 77, no. 1, pp. 49–68, 2011.

[14] G. Li, X. S. Li, L. G. Tang, and Y. Zhang, "Experimental investigation of production behavior of methane hydrate under ethylene glycol injection in unconsolidated sediment," *Energy & Fuels*, vol. 21, pp. 180–186, 2007.

[15] M. Kurihara, H. Ouchi, A. Sato et al., "Prediction of performances of methane hydrate production tests in the eastern Nankai Trough," in *Proceedings of the 7th International Conference on Gas Hydrates*, 2011.

[16] T. S. Collett, A. H. Johnson, C. C. Knapp, and R. Boswell, "Natural gas hydrates—a review," *Browse Collections*, vol. 89, pp. 146–219, 2009.

[17] G. J. Moridis, T. S. Collett, M. Pooladi-Darvish et al., "Challenges, uncertainties, and issues facing gas production from gas-hydrate deposits," *SPE Reservoir Evaluation and Engineering*, vol. 14, no. 1, pp. 76–112, 2011.

[18] N. Wu, H. Zhang, S. Yang et al., "Gas hydrate system of Shenhu area, Northern South China sea: geochemical results," *Journal of Geological Research*, 2011.

[19] X. Wang, T. S. Collett, M. W. Lee, S. Yang, Y. Guo, and S. Wu, "Geological controls on the occurrence of gas hydrate from core, downhole log, and seismic data in the Shenhu area, South China Sea," *Marine Geology*, vol. 357, pp. 272–292, 2014.

[20] S. Yang, M. Zhang, J. Liang et al., "Preliminary results of China's third gas hydrate drilling expedition: a critical step from discovery to development in the South China Sea," *Fire in the Ice*, vol. 15, pp. 1–5, 2015.

[21] X. Wang and D. Pan, "Application of AVO attribute inversion technology to gas hydrate identification in the Shenhu Area, South China Sea," *Marine and Petroleum Geology*, vol. 80, pp. 23–31, 2017.

[22] K. Zhang, G. J. Moridis, N. Wu, X. Li, and M. T. Reagan, "Evaluation of alternative horizontal well designs for gas production from hydrate deposits in the Shenhu area, South China Sea," in *Proceedings of the International Oil and Gas Conference and Exhibition in China 2010: Opportunities and Challenges in a Volatile Environment (IOGCEC '10)*, pp. 1417–1434, Society of Petroleum Engineers, June 2010.

[23] G. Li, G. J. Moridis, K. Zhang, and X.-S. Li, "Evaluation of gas production potential from marine gas hydrate deposits in Shenhu area of South China sea," *Energy & Fuels*, vol. 24, no. 11, pp. 6018–6033, 2010.

[24] Z. Su, Y. Cao, N. Wu, and Y. He, "Numerical analysis on gas production efficiency from hydrate deposits by thermal stimulation: application to the Shenhu Area, South China Sea," *Energies*, vol. 4, no. 2, pp. 294–313, 2011.

[25] Z. Su, Y. He, N. Wu, K. Zhang, and G. J. Moridis, "Evaluation on gas production potential from laminar hydrate deposits in Shenhu Area of South China Sea through depressurization using vertical wells," *Journal of Petroleum Science and Engineering*, vol. 86-87, pp. 87–98, 2012.

[26] Z. Su, G. J. Moridis, K. Zhang, and N. Wu, "A huff-and-puff production of gas hydrate deposits in Shenhu area of South China Sea through a vertical well," *Journal of Petroleum Science and Engineering*, vol. 86-87, pp. 54–61, 2012.

[27] J. Sun, F. Ning, S. Li et al., "Numerical simulation of gas production from hydrate-bearing sediments in the Shenhu area by depressurising: the effect of burden permeability," *Journal of Unconventional Oil & Gas Resources*, vol. 12, pp. 23–33, 2015.

[28] L. Huang, Z. Su, and N.-Y. Wu, "Evaluation on the gas production potential of different lithological hydrate accumulations in marine environment," *Energy*, vol. 91, pp. 782–798, 2015.

[29] Y. Yuan, T. Xu, X. Xin, and Y. Xia, "Multiphase flow behavior of layered methane hydrate reservoir induced by gas production," *Geofluids*, vol. 2017, Article ID 7851031, 15 pages, 2017.

[30] J. Sun, L. Zhang, F. Ning et al., "Production potential and stability of hydrate-bearing sediments at the site GMGS3-W19 in the South China Sea: a preliminary feasibility study," *Marine and Petroleum Geology*, vol. 86, pp. 447–473, 2017.

[31] J. Rutqvist and G. J. Moridis, "Coupled hydrologic, thermal and geomechanical analysis of well bore stability in hydrate-bearing sediments," in *Proceedings of the Offshore Technology Conference*, 2008.

[32] J. Rutqvist, G. J. Moridis, T. Grover, and T. Collett, "Geomechanical response of permafrost-associated hydrate deposits to depressurization-induced gas production," *Journal of Petroleum Science and Engineering*, vol. 67, no. 1-2, pp. 1–12, 2009.

[33] S. Uchida, K. Soga, A. Klar, and K. Yamamoto, "Geomechanical study of the Mallik gas hydrate production field trials," *Bulletin of the Geological Survey Canada*, vol. 601, pp. 191–204, 2012.

[34] M. Jiang, H. Chen, M. Tapias, M. Arroyo, and R. Fang, "Study of mechanical behavior and strain localization of methane hydrate bearing sediments with different saturations by a new DEM model," *Computers & Geosciences*, vol. 57, pp. 122–138, 2014.

[35] S. Uchida, A. Klar, and K. Yamamoto, "Sand production model in gas hydrate-bearing sediments," *International Journal of Rock Mechanics and Mining Sciences*, vol. 86, pp. 303–316, 2016.

[36] F. Wang, J. Jing, T. Xu, Y. Yang, and G. Jin, "Impacts of stratum dip angle on CO2 geological storage amount and security," *Greenhouse Gases: Science and Technology*, vol. 6, no. 5, pp. 682–694, 2016.

[37] F. Wang, J. Jing, Y. Yang et al., "Impacts of injection pressure of a dip-angle sloping strata reservoir with low porosity and permeability on CO2 injection amount," *Greenhouse Gases: Science and Technology*, vol. 7, no. 1, pp. 92–105, 2017.

[38] T. Fujii, K. Suzuki, T. Takayama et al., "Geological setting and characterization of a methane hydrate reservoir distributed at the first offshore production test site on the Daini-Atsumi Knoll in the eastern Nankai Trough, Japan," *Marine and Petroleum Geology*, vol. 66, pp. 310–322, 2015.

[39] K. Yamamoto, T. Kanno, X.-X. Wang et al., "Thermal responses of a gas hydrate-bearing sediment to a depressurization operation," *RSC Advances*, vol. 7, no. 10, pp. 5554–5577, 2017.

[40] X. Wang, M. Lee, T. Collett, S. Yang, Y. Guo, and S. Wu, "Gas hydrate identified in sand-rich inferred sedimentary section using downhole logging and seismic data in Shenhu area, South China Sea," *Marine and Petroleum Geology*, vol. 51, pp. 298–306, 2014.

[41] H. Wang, S. Yang, N. Wu, G. Zhang, J. Liang, and D. Chen, "Controlling factors for gas hydrate occurrence in Shenhu area on the northern slope of the South China Sea," *Science China Earth Sciences*, vol. 56, no. 4, pp. 513–520, 2013.

[42] R. Yang, P. Yan, N. Wu, Z. Sha, and J. Liang, "Application of AVO analysis to gas hydrates identification in the northern slope of the South China Sea," *Acta Geophysica*, vol. 62, no. 4, pp. 802–817, 2014.

[43] M. Su, R. Yang, H. Wang et al., "Gas hydrates distribution in the Shenhu area, Northern South China sea: comparisons between the eight drilling sites with gashydrate petroleum system," *Geologica Acta*, vol. 14, no. 2, pp. 79–100, 2016.

[44] M. Reagan, G. J. Moridis, T. Collett et al., "Toward production from gas hydrates: current status, assessment of resources, and simulation-based evaluationof technology and potential," *Spe Reservoir Evaluation & Engineering*, vol. 12, pp. 745–771, 2008.

[45] N.-Y. Wu, H.-Q. Zhang, S.-X. Yang, J. Liang, and H.-B. Wang, "Preliminary discussion on natural gas hydrate (NGH) reservoir system of Shenhu Area, north slope of South China Sea," *Natural Gas Industry*, vol. 27, pp. 1–6, 2007.

[46] X. Wang, D. R. Hutchinson, S. Wu, S. Yang, and Y. Guo, "Elevated gas hydrate saturation within silt and silty clay sediments in the Shenhu area, South China Sea," *Journal of Geophysical Research: Solid Earth*, vol. 116, no. 5, Article ID B05102, 2011.

[47] G. J. Moridis and M. Kowalsky, "Gas production from unconfined class 2 hydrate accumulations in the oceanic subsurface," *Economic Geology of Natural Gas Hydrate*, vol. 7, pp. 249–266, 2006.

[48] G. J. Moridis, S. Silpngarmlert, M. T. Reagan, T. Collett, and K. Zhang, "Gas production from a cold, stratigraphically-bounded gas hydrate deposit at the Mount Elbert Gas Hydrate Stratigraphic Test Well, Alaska North Slope: implications of uncertainties," *Marine and Petroleum Geology*, vol. 28, no. 2, pp. 517–534, 2011.

[49] G. J. Moridis and M. T. Reagan, "Gas production from class 2 hydrate accumulations in the permafrost," in *Proceedings of the SPE Annual Technical Conference and Exhibition 2007 (ATCE '07)*, pp. 3950–3976, Society of Petroleum Engineers, November 2007.

[50] J. Sun, F. Ning, L. Zhang et al., "Numerical simulation on gas production from hydrate reservoir at the 1st offshore test site in the eastern Nankai Trough," *Journal of Natural Gas Science and Engineering*, vol. 30, pp. 64–76, 2016.

[51] G. J. Moridis and M. T. Reagan, "Estimating the upper limit of gas production from Class 2 hydrate accumulations in the permafrost: 1. Concepts, system description, and the production base case," *Journal of Petroleum Science and Engineering*, vol. 76, no. 3-4, pp. 194–204, 2011.

[52] K. Yamamoto, Y. Terao, T. Fujii et al., "Operational overview of the first offshore production test of methane hydrates in the Eastern Nankai Trough," in *Proceedings of the Offshore Technology Conference 2014 (OTC '14)*, pp. 1802–1812, May 2014.

[53] M. T. van Genuchten, "A closed-form equation for predicting the hydraulic conductivity of unsaturated soils," *Soil Science Society of America Journal*, vol. 44, no. 5, pp. 892–898, 1980.

[54] J. Zhao, T. Yu, Y. Song et al., "Numerical simulation of gas production from hydrate deposits using a single vertical well by depressurization in the Qilian Mountain permafrost, Qinghai-Tibet Plateau, China," *Energy*, vol. 52, pp. 308–319, 2013.